An Improved Perturb and Observe MPPT for Photovoltaic Systems using Fuzzy Step Size

SALAH ANIS KRIM, FATEH KRIM, HAMZA AFGHOUL, FERIEL ABDELMALEK
University of Setif-1,
Faculty of Technology,
Laboratory of Power Electronics and Industrial Control, 19000 Setif,
ALGERIA

Abstract: - Photovoltaic (PV) systems have emerged as a promising energy resource that caters to the future needs of society, owing to their renewable, inexhaustible, and cost-free nature. The output power of these systems relies on solar cell radiation and temperature. To mitigate the dependence on atmospheric conditions and enhance power tracking, a conventional approach has been improved by integrating various methods. The Maximum Power Point Tracking (MPPT) algorithm is employed to optimize power extraction from PV systems. To overcome limitations such as steady-state voltage oscillations and improve transient response, two traditional MPPT methods, namely Perturb and Observe (P&O) and Fuzzy Logic Controller (FLC), have been modified. This research work aims to simulate and validate the fuzzy step size of the proposed modified P&O and FLC techniques within the MPPT algorithm using Matlab/Simulink™ for efficient power tracking in PV systems.

Key-Words: - Photovoltaic system; Matlab/Simulink; Perturb and Observe; MPPT; DC converter; Fuzzy.

Received: March 19, 2023. Revised: January 4, 2024. Accepted: February 17, 2024. Published: April 2, 2024.

1 Introduction

Research and development of alternative energy sources that are renewable, cleaner, and have less impact on the environment, have been prompted by the rising demand for energy and the potential for a reduction in the availability of traditional fuels, as evidenced by the petroleum, coal, and natural gas crisis, [1], [2], [3]. Additionally, among the alternative energy sources, the currently thought to be a more practical natural energy source is the generation of electrical energy from PV cells because it is plentiful, available for free, clean, and is dispersed throughout the earth. It also plays a crucial role in all other processes of energy production on Earth. Therefore, harnessing solar energy through PV cells has gained significant attention in the search for sustainable energy solutions. Besides, it is believed that solar energy incident on the Earth's surface is 10,000 times larger than global energy consumption, despite the phenomena of sunlight reflection and absorption by the atmosphere, [4].

Evaluation of a PV source due to its nonlinear output features which change with atmospheric temperature and solar irradiation are another crucial component of using a PV source. The characteristics become more complex, especially when the PV array receives non-uniform insolation, such as in partially shaded conditions, resulting in multiple peaks, [5]. The efficiency may reduce due to the existence of numerous peaks. Therefore, various methods have been developed to track the maximum power point (MPP), including the P&O algorithm and FLC, which are commonly used in PV systems.

The P&O algorithm can be presented by processing actual values of PV current and voltage, regardless of atmospheric circumstances, type of PV panel, or aging, to track the MPP continuously. Due to its easy implementation and simplicity, it has been a common method used in the PV system. The method involves perturbing the current or voltage of the PV array, either by decreasing or increasing its value, and comparing the resulting PV output power with the power from the previous perturbation cycle, [6]. The control system inclined the PV array operating point in that way if the operating voltage changes and the power increases; otherwise, the operating point is moved in the opposite direction. The next perturbation cycle of the algorithm is conducted in the same way. The benefits of the P&O method include its simplicity, ease of implementation and control, low cost, and high output power, [7], [8].

The FLC has also been widely adopted in PV systems to track the MPP because it is easy to develop, robust, and capable of tolerating

nonlinearity and working with imperfect inputs without the need for a precise mathematical model, [9], [10]. The FLC technique consists of three stages: fuzzification, aggregation, and defuzzification. A membership function is created during the fuzzification stage to convert the numerical input variables. The input and output systems are linguistically related. Rules are the relationships and a fuzzy set is the result of each rule. Therefore, numerous rules are applied to improve conversion efficiency. A separate output of a fuzzy set is created by aggregating the fuzzy sets produced by each rule, which is called as aggregation process. The defuzzification method subsequently sharpens the output from the fuzzy set, [11], [12], [13].

Driven by the literature survey mentioned earlier, in this paper, a modified method combining both the P&O algorithm and FLC has been developed. A modified fuzzy logic controller-based P&O for MPPT has been developed based on fuzzy variable step size due to limitations of traditional P&O approach such as delayed convergence or ascent to the MPP, oscillation of PV power around the MPP under steady state that results in loss power, and rapid changes in MPP position due to fluctuating atmospheric conditions. This paper is structured as follows. It consists of 5 parts, following the introduction, section 2 presents the PV system description which consists of the PV system, PV panel model, and power converter. Besides, section 3 presents the proposed Fuzzy Logic-based variable step size P&O MPPT, while section 4 consists of the discussion of the simulation outcomes and findings which are obtained from Matlab/Simulink™. Lastly, the conclusion is presented in section 5.

2 PV System Description

2.1 PV System

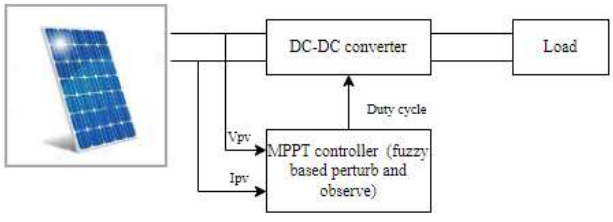

Fig. 1: Proposed PV System

Figure 1 illustrates the proposed PV system integrated with an MPPT controller. When designing a PV system, two key aspects need to be considered: the modeling of the MPPT boost DC-DC converter and the modeling of the PV array. The objective is to optimize power transmission by adjusting the load impedance to coincide with the operating point with the MPP, [14].

2.2 PV Panel Model

Electrical energy can be generated through the conversion of solar energy, facilitated by solar PV technologies. These technologies rely on solar cells to directly convert sunlight exposure into electrical energy in the form of direct current (DC). Figure 2 illustrates the circuit model of a PV panel, which comprises diodes, resistors, and a current source. PV cells employ a semiconductor structure, typically a p-n junction, to harness the energy from photons in sunlight. When exposed to solar radiation, the cells absorb photons, causing the mobilization of electrons and the subsequent generation of electricity. As a result, when a load is connected to a PV cell during the period of irradiance, electric charges flow as direct current. To achieve the desired current and voltage levels, the cells can be connected in either parallel or series configurations. Connecting the cells in series allows for higher output voltage while connecting them in parallel enables higher output current

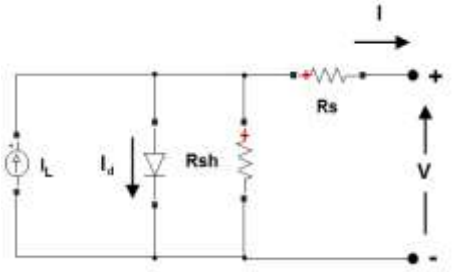

Fig. 2: PV array modeling circuit

Figure 2 illustrates the circuit model of the PV array, which enables the determination of I_{pv} representing the output current of the PV array. Equ. (1) provides the derivation of $I_{p\square}$, which represents the photogenerated current and is expressed as follows:

$$I_{ph} = \left(I_{sc} + k_i(T_c - T_{stc})\right)\left(\frac{G}{G_{stc}}\right) \quad (1)$$

Where I_{sc} is the short circuit current of PV system, k_i is the short circuit current coefficient, T_c is the absolute operating temperature, T_{stc} is the temperature at standard test condition (STC) @ 25°C, G is the irradiance and G_{stc} is the irradiance at standard test condition (STC) @ 1000W/m². But, in indoor cconditions the $I_{p\square} \approx 0$, where the I-V characteristics of the PV array is expressed by Equs. 2, 3, 4 as:

$$I_{pv} = I_{cs} - I_o\left(e^{\frac{V_{pv}-I_{pv}R_S}{N_S V_t}} - 1\right) - I_{sh} \quad (2)$$

$$V_{pv} = \left(I_{cs} - I_{pv}\right)R_s + nV_t ln\frac{(I_{cs}-I_{pv})-I_{sh}+I_o}{I_o} \quad (3)$$

$$I_{sh} = \frac{V_{pv}-(I_{cs}-I_{pv})R_s}{R_{sh}} \quad (4)$$

Where, I_o represents the dark saturation current, I_{cs} is the output current, R_s is the panel series resistance, R_{s} is the panel shunt or parallel resistance, N_s is the number of cells connected in series, V_t is the junction thermal voltage that is given by equation of $V_t = kT_c/q$, where k is the Boltzmann's constant of $1.381 \times 10^{-23}\,J/K$ and q is the elementary charge of $1.602 \times 10^{-19}\,C$. The parameters of the PV array under STC are presented in Table 1.

Table 1. Parameters of the solar panel 1 Soltech 1STH-250-WH at STC

Electrical Characteristics	Parameters
Rated maximum power (P_{max})	250.205W
Open-circuit voltage (V_{oc})	37.3V
Short-circuit current (I_{sc})	8.66A
Voltage at MPP (V_{mpp})	30.7V
Current at MPP (I_{mpp})	8.15A
Voltage temperature coefficient	-0.36901%/°C
Current temperature coefficient	0.086998

2.3 Power Converter

Power electronics is essentially employed in PV panels, wind turbines, and geothermal resources which need power conditioning systems, improve grid integrations. Energy conversions phenomena occur to be usable and user-friendly. For example consider a PV generator which provides DC power, to obtain AC power here a power electronic converter called inverter is used. A power converter is a power electronic circuit that receives a DC input and generates a DC output with different voltage. This transformation is achieved through high-frequency switching actions that involve inductive and capacitive filter elements. The purpose of a power converter is to convert electrical energy from one form to an optimized form that suits the specific load requirements. In the context of PV systems, one commonly used type of power converter is the DC-DC boost converter, [15]. Figure 3 illustrates the basic configuration of a DC-DC boost converter. It comprises two semiconductor devices, such as a transistor and a diode/IGBT, as well as an inductor, input and output capacitors, and a DC load connection. The boost converter operates by increasing the input DC voltage, making it a step-up converter, as the output voltage is greater than the source voltage, [16].

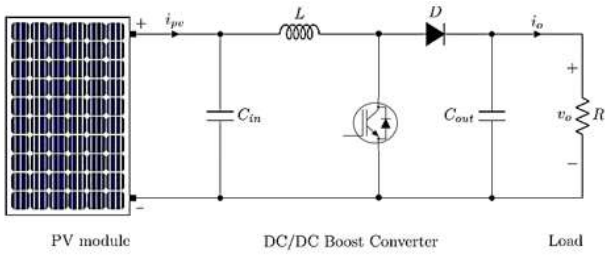

Fig. 3: DC-DC boost converter

The equation of the DC-DC boost converter is derived as follows, where the boost level of the output voltage is determined by the duty ratio of the switch and the applied input voltage:

$$V_o = V_i(1 - D) \quad (5)$$

When the condition of the IGBT/diode is on and D is reverse biased in (6), (7) and (8), the output voltage is obtained from the derivation input voltage and duty cycle from the equation below:

$$\frac{di_L}{dt} = \frac{V_{pv}}{L} \quad (6)$$

$$\frac{dV_o}{dt} = -\frac{V_o}{RC_{out}} \quad (7)$$

$$I_{pv} = i_L + C_{in}\frac{dV_{pv}}{dt} \quad (8)$$

Equs. (9), (10) are derived by correlating the relationship between the changing of inductor current with time and PV voltage with inductor when the condition of IGBT/diode turned off and D is forward biased.

$$\frac{di_L}{dt} = \frac{V_{pv}}{L} - \frac{V_o}{L} \quad (9)$$

$$\frac{dV_o}{dt} = \frac{i_L}{C_{out}} - \frac{V_o}{RC_{out}} \quad (10)$$

By altering the duty cycle D, the power converter is in charge of controlling the energy transmission from the input source to the load. Since in steady state the integral of the induction voltage over one time period must be zero, we obtain Equ. 11. Equ. (12) shows the simplified version of Equ. (11), where PV voltage of cell is excluded.

$$V_{pv}t_{on} = \left(V_o - V_{pv}\right) \times t_{off} \quad (11)$$

$$V_o = \frac{t_{on}+t_{off}}{t_{off}}V_{pv} \quad (12)$$

$$T = t_{on} + t_{off} \quad (13)$$

The general equation of period is stated in (13) where the turn-on time is summed with the turn-off time. Then, Equ. (14) represents the ratio of turn on time to period called as duty cycle, a.

$$D = \frac{t_{on}}{T} \quad (14)$$

Then, from Equ. (12), the voltage produced can be derived as (15) where the output voltage is determined from the input voltage of the solar cell and duty cycle.

$$V_o = \frac{1}{1-D} Vpv \quad (15)$$

3 Fuzzy Logic based Variable Step Size P&O for MPPT

3.1 Perturb and Observe Description

P&O techniques are commonly employed to extract the maximum power point in a PV system due to their simplicity and minimal parameters requirement. The voltage of the array is periodically perturbed by either increasing or decreasing it, and the P&O algorithm compares the PV output power with the power from the previous perturbation cycle, [17]. If the power increases, the perturbation continues in the same direction; otherwise, it changes direction. As a result, each MPPT cycle induces a change in the terminal voltage of the array. In situations where atmospheric conditions exhibit continuous or gradual changes, the P&O algorithm will subsequently adapt, potentially leading to a loss of PV power, [18].

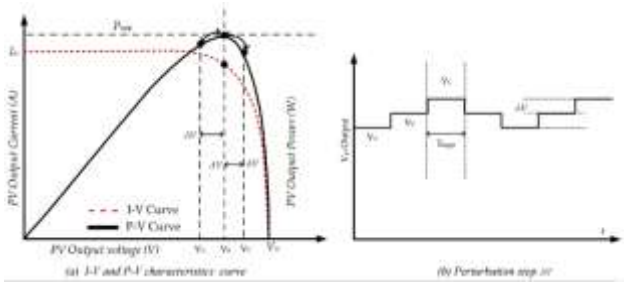

Fig. 4: P&O MPPT operation

Figure 4 illustrates the operation of P&O MPPT, taking into account the I-V and P-V characteristics curves and the step size of voltage perturbation. It clearly demonstrates that the electrical behavior of a solar PV system under varying solar irradiance is described by the output current and voltage. The MPP is achieved when the terminal voltage of the PV source is effectively controlled to maintain a value that maximizes the product of PV current and voltage. As shown in Figure 4, the knee point of the standard I-V curve for PV diodes is indicated, with the limits displayed for short circuit current (I_{sc}) and open circuit voltage (V_{oc}), [19].

The basic concept behind the P&O approach for MPPT is to analyze the voltage and output power derivatives of the PV array, which determine the shift in the operating point. This method involves periodically adjusting the PV array voltage by either increasing or decreasing it. If an increase in the operating voltage leads to a rise in output power, the operating point will be located to the left of the MPP, necessitating further voltage perturbations to reach the MPP on the right side. On the other hand, if an increase in voltage results in a decrease in power, the operating point will be positioned to the right of the MPP, requiring additional perturbations to move towards the left side and approach the MPP, [20], [21].

3.2 Fuzzy Logic Controller Description

The FLC is a well-known artificial intelligence-based control technique used in MPPT. Fuzzy logic, or fuzzy set theory, is a novel approach to achieving peak power point tracking. In Figure 5, the block diagram of the FLC illustrates the mapping of input variables, such as the first perturbation step size and the instantaneous measured slope of PV power, into linguistic values through fuzzification. This process involves the use of linguistic variables and fuzzy sets, which represent smooth changes in membership rather than abrupt transitions, forming the basis for fuzzy logic controllers, [22]. The inference engine in the controller assesses the fuzzy rules and linguistic variable definitions to make decisions and determine the appropriate fuzzy control action. To obtain a non-fuzzy (crisp) control action that closely resembles the fuzzy one, a defuzzification technique is applied since a fuzzy controller produces a fuzzy set as its output. The final step involves obtaining the crisp value for the variable step size, as the output of the controller.

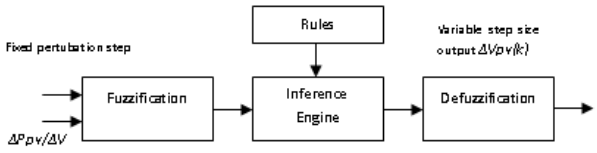

Fig. 5: Fuzzy logic controller block diagram

FLC is a heuristic approach that allows the incorporation of human thinking and knowledge into the design of nonlinear controllers, [23]. Typically, fuzzy controller rules are expressed using linguistic terms. There are two types of fuzzy inference systems commonly used: Mamdani and Sugeno. The Mamdani inference system synthesizes a collection of linguistic control rules defined by

expert human operators, with each rule producing a fuzzy set as its output. This system is particularly suitable for expert system applications, such as medical diagnostics, where the rules are based on human expertise and are relatively straightforward to understand, [24]. On the other hand, the Sugeno inference system, also known as the Takagi-Sugeno-Kang inference, uses singleton output membership functions that can be either linear functions or constants of the input values. Unlike the Mamdani system, which computes the centroid of a two-dimensional area, a Sugeno system employs a weighted sum or average of a small number of data points, making it more computationally efficient, [25].

Table 2 shows the fuzzy rules table for MPPT. There are about 25 rules developed in the fuzzy logic toolbox to prescribe the conclusion of the instantaneous voltage of the variable step size. The inputs indicate the step size perturbation and P-V curve slope while one output indicates variable step size.

Table 2. Fuzzy rules table for MPPT

Δe = S(k) *E = Voltage Step*	PVS	PS	PM	PH	PVH
PVS	PVH	PVS	PVS	PS	PS
PS	PVH	PVS	PVS	PS	PS
PM	PS	PS	PS	PVH	PVH
PH	PS	PS	PVH	PVH	PVH
PVH	PVS	PVS	PVH	PVH	PVH

where PVS = Positive Very Small, PS = Positive Small, PM = Positive Medium, PH = Positive High and PVH = Positive Very High

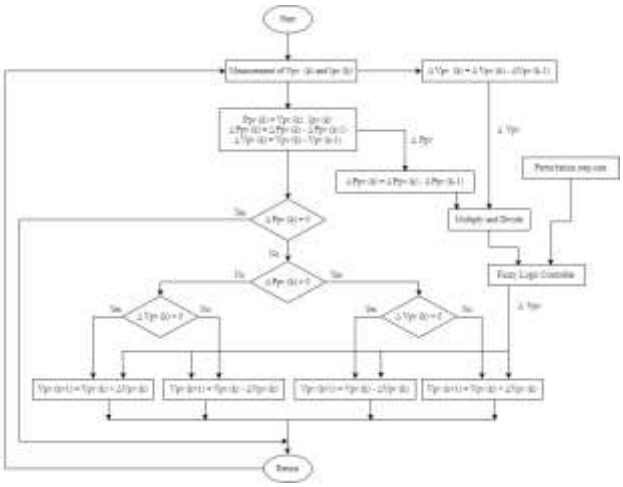

Fig. 6: Flowchart of the proposed FLC-based P&O

Figure 6 illustrates the flowchart of the proposed FLC-based P&O algorithm. This later evaluates power variations and adjusts the operational voltage of a PV system by modifying the effective input resistance of the boost converter through the duty cycle adjustment of the switching device. The system initiates by measuring two parameters: voltage and current from the PV system. The flowchart provides a detailed explanation of the process.

Firstly, the voltage and current measurements lead to two distinct paths: the P&O method and FLC. Various calculations are performed based on the measurements to determine the actual power (Ppv (k)), the changes in power (Δ Ppv (k)), and the changes in voltage (Δ Vpv (k)). These calculations involve combining the instantaneous current and voltage values with their respective previous values. The FLC receives two inputs: the slope, which is the result of the division between ΔP and ΔV, and the perturbation step size.

The output of the FLC is the variable step size for making small changes in voltage, which is added to the PV voltage. This action also modifies the duty cycle of the PV voltage based on the two inputs. The PV panel is considered to operate at the MPP condition when the delta power equals zero. When ΔP is greater than zero, the sign is positive, and vice versa. Similarly, when ΔV is positive, the voltage is updated by adding the small changes derived from the output of the FLC. The design of fuzzy logic-based P&O for PV MPPT is implemented and simulated in Matlab/Simulink and is discussed in the following section.

4 Outcomes and Discussion

4.1 PV System Circuit Model

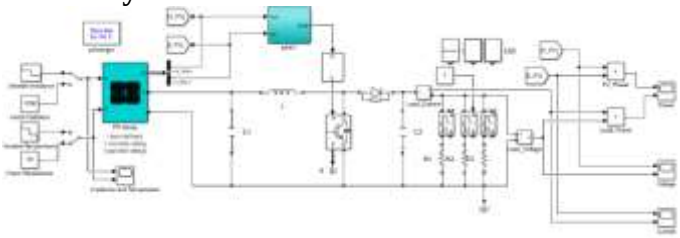

Fig. 7: A circuit simulation model

The PV system circuit model is then presented using Matlab/Simulink™ software to determine system performance based on variable conditions. The model consists of a PV model of 1Soltech 1STH-250-WH, a boost converter, loads, and fuzzy logic controller-based P&O MPPT algorithm,

Figure 7. The PV array with a capacity of 250.205W consists of one series modules and one parallel string. The loads considered in this model are 5Ω, 30Ω, and 100Ω while the power converter used is IGBT with diode boost converter.

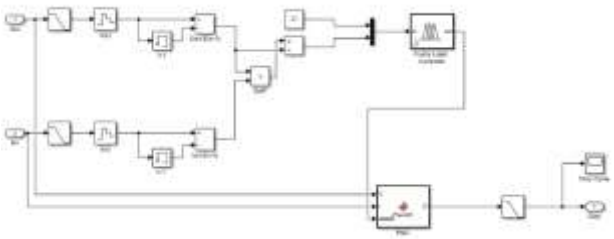

Fig. 8: MPPT controller subsystem

4.2 Fuzzy Rule

The fuzzy rule is constructed using the fuzzy logic designer in Matlab/Simulink™, as shown in Figure 8. The membership functions involve two input variables and one output variable for the FIS. The first input variable represents the perturbation step size, labeled as FS and depicted in Figure 9. The second input, denoted as S in Figure 10, corresponds to the slope of the P-V curve or ΔP/ΔV. The fuzzy logic controller generates an output called the variable step size (VSS), as illustrated in Figure 11.

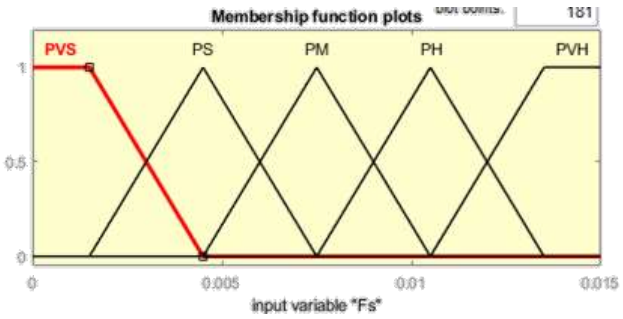

Fig. 9: Input variable of perturbation step size, FS

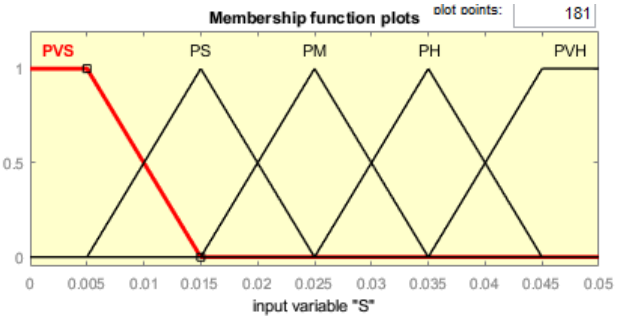

Fig. 10: Input variable of P-V curve slope, S

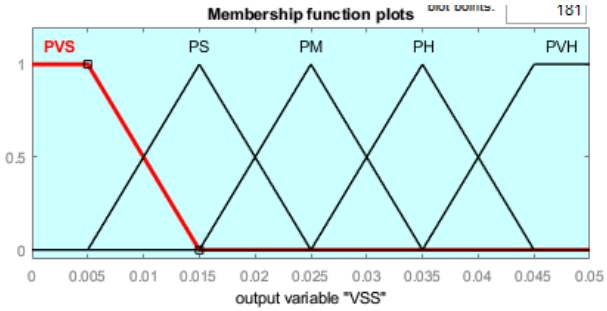

Fig. 11: Output variation of variable step size, VSS

When the design of fuzzy logic is finished, the rules and surface viewer are presented in Figure 12 and Figure 13, respectively. There are 25 different rules corresponding between the inputs and output of FIS variables. An example of an if-then rule is stated below:

1. If (A is X1) and (B is Y1) then (C is A1)

……

25. If (A is X5) and (B is Y5) then (C is A25)

where A = First input, X1 = First variable of first input, B = Second input, Y1 = First variable of second input, C = Output, A1 = First output and A25 = 25th output.

The fuzzy rule consists of fixed variables A, B, and C, along with changing variables X1, Y1, and A1~A25, which represent the variable relationship according to the fixed variables. These rules are visualized in a 3-D dimension due to the presence of three different FIS variables, as shown in Figure 12. The complete set of rules can be seen in the rule viewer depicted in Figure 13. The inference process of the fuzzy system involves adjusting the two inputs to observe the corresponding output for each fuzzy rule, including the aggregated output fuzzy set and defuzzified output values. The output of the fuzzy logic controller represents the change in the duty cycle (ΔD), which completes the P&O algorithm. Therefore, this method is designed in the proposed Fuzzy Logic-based P&O approach to ensure that the PV output always remains in an optimal state.

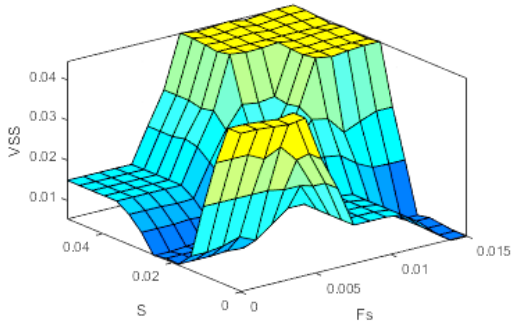

Fig. 12: 3D Dimensions of fuzzy rule

4.3 Fuzzy Rule

4.3.1 P-V and I-V curves

The graphs of Figure 14 and Figure 15 are plotted using the parameters of the 1Soltech 1STH-250-WH array and are displayed for two specific conditions: array @ 25°C with specified irradiances and array @ 1000 W/m² with specified temperatures. Various irradiance and temperature values are examined to track different states of the maximum power point. In Figure 14, the irradiance levels are varied from 1000 W/m² to 400 W/m², while in Figure 15, the temperatures range from 85°C to 25°C. The red dot indicates the maximum power point and the corresponding maximum current at different voltages. These curves are correlated with the simulation results of the PV system circuit model. Furthermore, a comparison is made between the outputs of the boost converter with loads and the input of PV power.

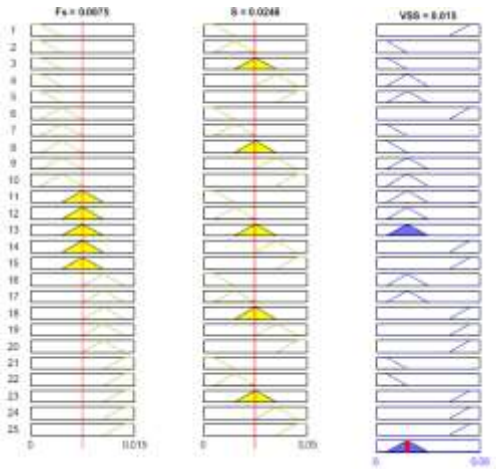

Fig. 13: Rule viewer in MATLAB windows of fuzzy logic

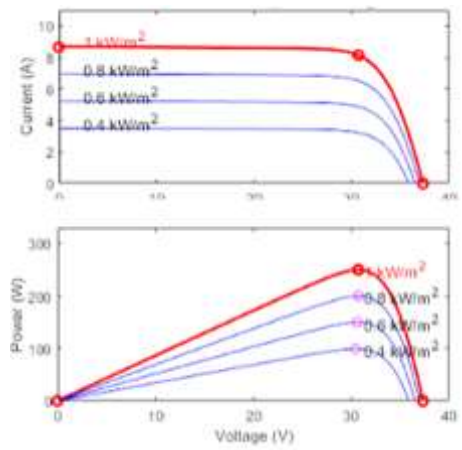

Fig. 14: I-V and P-V curve characteristics for changing irradiance and fixed temperature

4.3.2 Changing Irradiance and Fixed Temperature

Figure 16 represent irradiance and temperature profiles. We focus on the changing irradiance with a fixed temperature of 25°C. The blue line in Figure 17, Figure 18 and Figure 19 represents the PV array's initial condition, while the red line represents the boost and load variables.

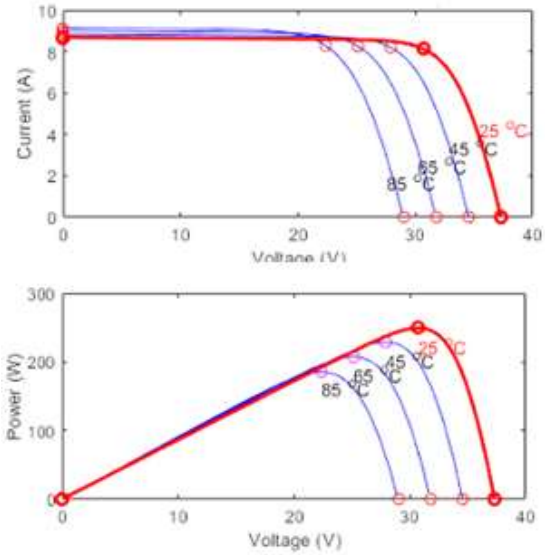

Fig. 15: I-V and P-V curve characteristics for changing temperature and fixed irradiance

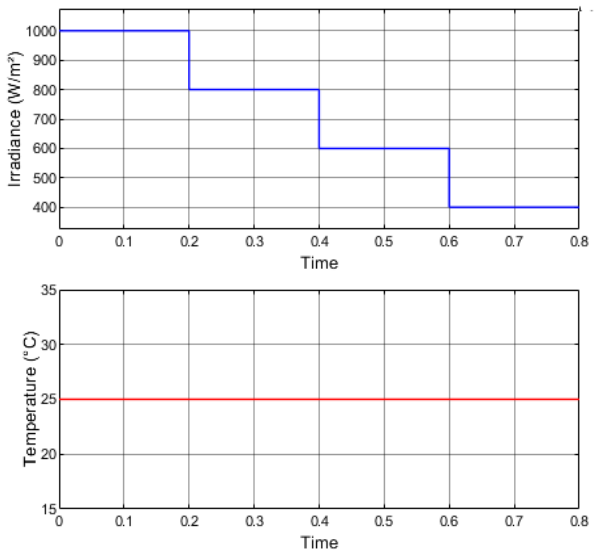

Fig. 16: Changing irradiance and fixed temperature

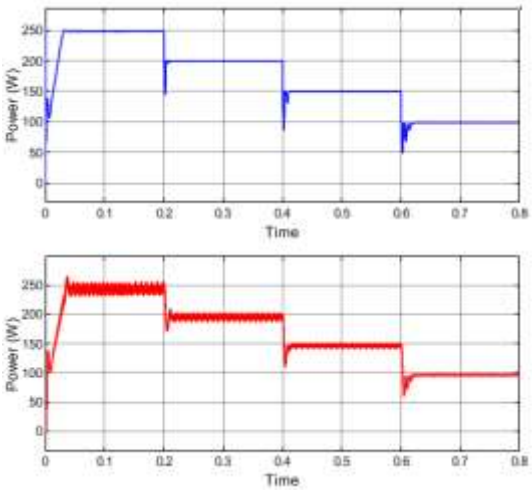

Fig. 17: PV power and load power

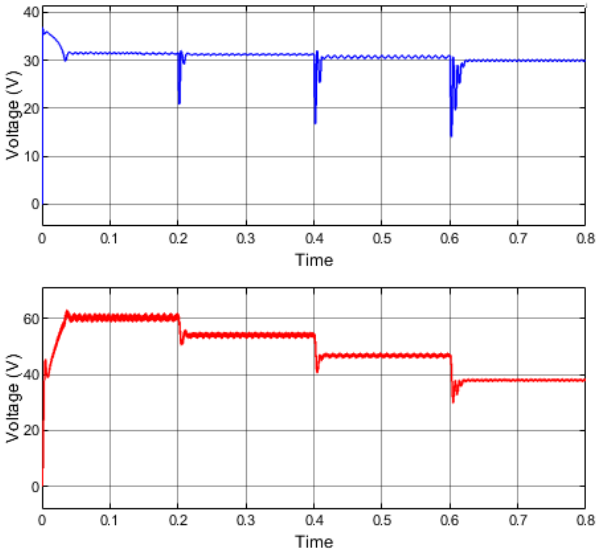

Fig. 18: PV voltage and load voltage

Figure 17 shows a "ladder down-shape" profile, indicating that the PV power varies with the different irradiance levels.

At t = 0.1 s, when the irradiance is 1000 W/m², the power at the maximum power point is approximately 250 W. However, when the irradiance decreases to 800 W/m² at t = 0.2 s, the power drops to around 200 W due to reduced irradiance reception. Both graphs demonstrate similar outputs in controlling the PV power to maintain stability and avoid voltage fluctuations.

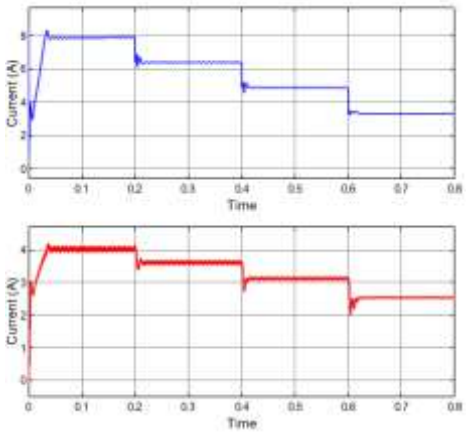

Fig. 19: PV current and load current

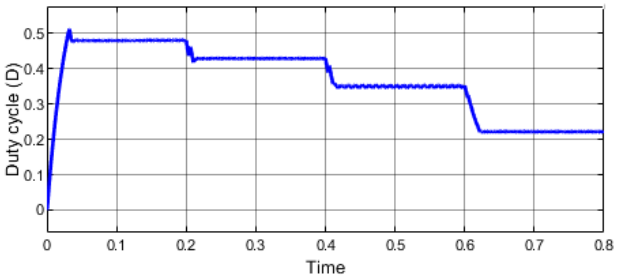

Fig. 20: Duty ration change with irradiation

Table 3. Key results

	Irradiance (W/m²) and 25°C							
	1000		800		600		400	
	PV	Load	PV	Load	PV	Load	PV	Load
P (W)	247	247	199	198	149	149	98.	98
V (V)	31	60	31	54	30	47	29	38
I (A)	7.85	4.064	6.388	3.636	4.827	3.153	3.298	2.56
D	0.4808		0.4305		0.3502		0.2198	

The explanation for these power outputs is provided in Figure 18 and Figure 19. Figure 18 shows that at an irradiance of 1000 W/m², the PV voltage is 31.54 V, while the load voltage is 60.95 V, as a result of the boost converter's nature to step up the system voltage. Similarly, Figure 19 illustrates that the PV current is 7.85 A, and the load current is 4.064 A, which is less than the input current due to the voltage increase in the boost converter at 1000 W/m². This relationship aligns with Ohm's Law, where power is the product of voltage and current, as stated in the P&O subsystem. To achieve the maximum power point, the voltage or current needs to increase or decrease simultaneously. Hence, when the voltage reaches its maximum or rises, the current decreases. Finally, Figure 20 shows the variation of the duty ratio, which follows the irradiance level. The initial duty

cycle is 0.4808 and decreases proportionally with decreasing irradiance, Table 3.

Hence, the simulation results indicate that the proposed modified P&O-based fuzzy logic controller exhibits excellent system performance by minimizing steady-state oscillations near the maximum power point and demonstrating a prompt response to variations in irradiance.

5 Conclusion

PV is undeniably one of the most significant alternative methods for generating renewable energy. However, a PV system without an MPPT algorithm faces challenges in harnessing the maximum power potential. An MPPT algorithm is essential to ensure that the PV array operates at its maximum power point. In this regard, an enhanced P&O MPPT algorithm, incorporating a fuzzy logic controller with a variable step size, was developed and implemented to overcome the limitations of the traditional fixed step size approach. Simulation results demonstrate that the proposed method reduces steady-state oscillations around the MPP and exhibits a faster response to changes in irradiance. The main objectives of this work were to evaluate and simulate the variable step size modifications of the P&O algorithm in a PV system. Three criteria were analyzed, including power generated, current, voltage, and duty cycle, by comparing them with the P-V and I-V curve characteristics of the PV panel. The results reveal a trade-off between minimizing convergence time towards the maximum power point and reducing oscillations in the photovoltaic array's power output around the maximum power point, addressing some of the drawbacks associated with using a fixed step size in MPPT. Consequently, the primary goal of this paper, which aimed to examine the effectiveness of the modified P&O-based fuzzylogic controller with a variable step size in a PV system, has been achieved. In future work, MPPT with the hybrid HBA-COA technique will be evaluated on an experimental hardware platform using a PV emulator. MPPT based on deep learning will be developed and compared to the proposed technique.

References:

[1] M. A. Abo-Sennah, M. A. El-Dabah, and M. A. El-Biomey, "Maximum power point tracking techniques for photovoltaic systems: a comparative study," *International Journal of Electrical & Computer Engineering*, vol. 11, no. 1, pp. 2088–8708, 2021.

[2] L. Abualigah, R. A. Zitar, K. H. Almotairi, A. M. Hussein, M. Abd Elaziz, M. R. Nikoo, and A. H. Gandomi, "Wind, solar, and photovoltaic renewable energy systems with and without energy storage optimization: A survey of advanced machine learning and deep learning techniques," *Energies*, vol. 15, no. 2, pp. 578, 2022.

[3] R. Kumar, and S. K. Singh, "Solar photovoltaic modeling and simulation: As a renewable energy solution," *Energy Reports*, vol. 4, pp. 701–712, 2018.

[4] S. S. Nadkarni, S. Angadi, and A. B. Raju, "Simulation and Analysis of MPPT Algorithms for Solar PV based Charging Station," Conference: *2018 International Conference on Computational Techniques, Electronics and Mechanical Systems (CTEMS)*, pp. 45–50, 2018.

[5] B. E. Elnaghi, M. E. Dessouki, M. N. Abd-Alwahab, and E. E. Elkholy, "Development and implementation of two-stage boost converter for single-phase inverter without transformer for PV systems," *International Journal of Electrical & Computer Engineering*, vol. 10, no. 1, pp. 2088–8708, 2022.

[6] A. Mohapatra, B. Nayak, and C. Saiprakash, "Adaptive perturb & observe MPPT for PV system with experimental validation," *in 2019 IEEE International Conference on Sustainable Energy Technologies and Systems (ICSETS)*, Feb. 2019, pp. 257–26.

[7] D. Pilakkat and S. Kanthalakshmi, "Study of the Importance of MPPT Algorithm for Photovoltaic Systems under Abrupt Change in Irradiance and Temperature Conditions," *WSEAS Transactions on Power Systems*, vol.15, pp. 8-20, 2020, https://doi.org/10.37394/232016.2020.15.2.

[8] B. Sankar, A. Yappan and R. Seyezhai, "Comparative analysis of Maximum Power Point Tracking Algorithms for photovoltaic applications," *WSEAS Transactions on Power Systems*, vol.15, pp. 161-171, 2020, https://doi.org/10.37394/232016.2020.15.20.

[9] A. S. Samosir, H. Gusmedi, S. Purwiyanti, and E. Komalasari, "Modeling and simulation of fuzzy logic based maximum power point tracking (MPPT) for PV application," *Int. J. Electr. Comput. Eng.*, vol. 8, no. 3, pp. 1315–1323, 2018.

[10] A. Al-Gizi, A. H. Miry, and M. A. Shehab, "Optimization of fuzzy photovoltaic maximum power point tracking controller

using chimp algorithm," *International Journal of Electrical & Computer Engineering*, vol. 12, no. 5, pp. 2088–8708, 2023.

[11] N. K. Pandey, R. K. Pachauri, S. Choudhury, and R. K. Sahu, "Asymmetrical interval Type-2 Fuzzy logic controller based MPPT for PV system under sudden irradiance changes," *Materials Today: Proceedings*, vol. 80, pp. 710–716, 2023.

[12] R. Arulmurugan, "Optimization of perturb and observe based fuzzy logic MPPT controller for independent PV solar system," *WSEAS Transactions on Power Systems*, vol. 19, pp. 159-167, 2020, https://doi.org/10.37394/23202.2020.19.21.

[13] S. D. Al-Majidi, M. F. Abbod, and H. S. Al-Raweshidy, "A Modified P&O-MPPT based on Pythagorean Theorem and CV-MPPT for PV Systems," *in 2018 53rd International Universities Power Engineering Conference (UPEC)*, Sept. 2018, pp. 1–6.

[14] Z. M. S. Elbarbary, and M. A. Alranini, "Review of maximum power point tracking algorithms of PV system," *Frontiers in Engineering and Built Environment*, vol. 1, no. 1, pp. 68-80, 2021.

[15] R. Arulmurugan, "Comparative evaluation of new FLC controller based MPPT for a DC to DC buck-boost zeta converter," *WSEAS Transactions on Power Systems*, vol.11, pp.27-34, 2016.

[16] U. Yilmaz, A. Kircay, and S. Borekci, "PV system fuzzy logic MPPT method and PI control as a charge controller," *Renewable and Sustainable Energy Reviews*, vol. 81, pp. 994–1001, 2018.

[17] S. Singh, S. Manna, M. I. H. Mansoori, and A. K. Akella, "Implementation of perturb & observe MPPT technique using boost converter in PV system," *in 2020 International Conference on Computational Intelligence for Smart Power System and Sustainable Energy (CISPSSE)*, July 2020, pp. 1–4.

[18] M. Jiang, M. Ghahremani, S. Dadfar, H. Chi, Y. N. Abdallah, and N. Furukawa, "A novel combinatorial hybrid SFL–PS algorithm based neural network with perturb and observe for the MPPT controller of a hybrid PV-storage system," *Control Engineering Practice*, vol. 114, pp. 104880, 2021.

[19] N. Kumar, I. Hussain, B. Singh, and B.K. Panigrahi, "Framework of Maximum Power Extraction From Solar PV Panel Using Self Predictive Perturb and Observe Algorithm," *IEEE Trans. Sustain. Energy* 2018, vol. 9, pp. 895–903.

[20] M. N. Ali, K. Mahmoud, M. Lehtonen, and M. M. Darwish, "An efficient fuzzy-logic based variable-step incremental conductance MPPT method for grid-connected PV systems," *IEEE Access*, vol. 9, pp. 26420–26430, 2021.

[21] M.A. Abdourraziq, M. Maaroufi, M. Ouassaid and M. Tlemcani "Maximum Power Point Tracking Method Based Fuzzy Logic Control for Photovoltaic Systems," *WSEAS Transactions on Power Systems*, Vol. 12, pp. 324-334, 2017.

[22] X. Li, Q. Wang, H. Wen, and W. Xiao, "Comprehensive studies on operational principles for maximum power point tracking in photovoltaic systems," *IEEE Access*, vol. 7, pp. 121407–121420, 2019.

[23] José Fernando Silva, Sónia F. Pinto, "*Linear and Nonlinear Control of Switching Power Converters*", Power Electronics Handbook (Fourth Edition).

[24] Mamdani, E.H., and S. Assilian. "An Experiment in Linguistic Synthesis with a Fuzzy Logic Controller," *International Journal of Man-Machine Studies* 7, no. 1 (January 1975): 1–13.

[25] M. Sugeno, *Industrial Applications of Fuzzy Control*, Amsterdam, New York, N.Y., U.S.A, Elsevier Science Pub. Co, 1985.

Contribution of Individual Authors to the Creation of the Article

- Salah Anis Krim carried out the design of the system.
- Hamza Afghoul achieved the simulation of the system.
- Fateh Krim proposed an improved algorithm.
- Feriel Abdelmalek achieved the discussion of the outcomes.

Sources of Funding for Research Presented in a Scientific Article or Scientific Article Itself

No funding was received for conducting this study.

Conflict of Interest

The authors have no conflicts of interest to declare.